The Plant Cell, Vol. 23: 3247–3259, September 2011, www.plantcell.org

WOX4 Imparts Auxin Responsiveness to Cambium Cells in *Arabidopsis* [C][W][OA]

Stefanie Suer, Javier Agusti, Pablo Sanchez, Martina Schwarz, and Thomas Greb[1]

Gregor Mendel Institute of Molecular Plant Biology, Austrian Academy of Sciences, 1030 Vienna, Austria

Multipotent stem cell populations, the meristems, are fundamental for the indeterminate growth of plant bodies. One of these meristems, the cambium, is responsible for extended root and stem thickening. Strikingly, although the pivotal role of the plant hormone auxin in promoting cambium activity has been known for decades, the molecular basis of auxin responsiveness on the level of cambium cells has so far been elusive. Here, we reveal that auxin-dependent cambium stimulation requires the homeobox transcription factor WOX4. In *Arabidopsis thaliana* inflorescence stems, 1-*N*-naphthylphthalamic acid–induced auxin accumulation stimulates cambium activity in the wild type but not in *wox4* mutants, although basal cambium activity is not abolished. This conclusion is confirmed by the analysis of cellular markers and genome-wide transcriptional profiling, which revealed only a small overlap between *WOX4*-dependent and cambium-specific genes. Furthermore, the receptor-like kinase PXY is required for a stable auxin-dependent increase in *WOX4* mRNA abundance and the stimulation of cambium activity, suggesting a concerted role of *PXY* and *WOX4* in auxin-dependent cambium stimulation. Thus, in spite of large anatomical differences, our findings uncover parallels between the regulation of lateral and apical plant meristems by demonstrating the requirement for a WOX family member for auxin-dependent regulation of lateral plant growth.

INTRODUCTION

Plants have the capacity to adapt their growth dynamics to changing environmental conditions, a competence representing an adaptation to their sessile life style. This developmental plasticity is based on the activity of indeterminate groups of stem cells, the meristems, which constantly integrate environmental and endogenous signals, ensuring coordinated growth of tissues and organs. Secondary growth, the lateral expansion of growth axes predominantly in gymnosperms and in dicotyledonous plants, is one example of a growth process that is under tight control of endogenous and environmental cues (Elo et al., 2009). It depends on the activity of the cambium, a meristem located at the periphery of stems and roots. The cambium produces water-conducting xylem tissue (wood) centripetally and assimilates conducting phloem tissue (bast) centrifugally, resulting in an increase of both transport capacity along growth axes and mechanical support for extended root and shoot systems.

Initially observed in the first half of the last century (Snow, 1935), it is well established that shoot apex–derived auxin, which is transported basipetally along the stem, is essential for secondary stem growth (Little et al., 2002; Ko et al., 2004; Björklund et al., 2007). In fact, measurements in the stem of *Pinus sylvestris* and *Populus* along the radial sequence of tissues show that auxin concentration peaks in the cambium, and it has been suggested that radial concentration gradients mediate positional information essential for the establishment of cell identities (Uggla et al., 1996, 1998; Schrader et al., 2003). However, most genes whose expression patterns correlate with the radial auxin gradient are not auxin responsive, questioning a strong and direct impact of auxin levels on radial patterning (Nilsson et al., 2008). The expression of genes involved in auxin transport, such as members of the AUX1-like family of auxin influx carriers or the PIN family of auxin efflux carriers, is likewise found in radial gradients, showing that auxin distribution is correlated with auxin transport (Schrader et al., 2003). Interestingly, absolute auxin levels in the active and dormant cambium in trees are similar, suggesting an annual fluctuation of auxin sensitivity (Uggla et al., 1996; Schrader et al., 2003, 2004a). Indeed, reduced auxin responsiveness of the dormant cambium correlates with reduced expression levels of components of the auxin perception machinery, implying that altering auxin responsiveness serves as a major mechanism regulating cambium activity (Baba et al., 2011).

In root apical meristems (RAMs), an auxin maximum is present in the quiescent center, declining toward more differentiated cells (Sabatini et al., 1999; Petersson et al., 2009). This particular auxin distribution is essential for root patterning and for maintaining stem cell identities (Sabatini et al., 1999; Friml et al., 2002; Blilou et al., 2005; Ding and Friml, 2010). The WUSCHEL-RELATED HOMEOBOX5 (WOX5) transcription factor is specifically expressed in the quiescent center, where it is important for maintaining the stem cell character of neighboring cells (Sarkar et al., 2007). Several lines of evidence suggest a role for *WOX5* downstream of auxin in regulating distal stem cell dynamics. The

[1] Address correspondence to thomas.greb@gmi.oeaw.ac.at.
The author responsible for distribution of materials integral to the findings presented in this article in accordance with the policy described in the Instructions for Authors (www.plantcell.org) is: Thomas Greb (thomas.greb@gmi.oeaw.ac.at).
[C]Some figures in this article are displayed in color online but in black and white in the print edition.
[W]Online version contains Web-only data.
[OA]Open Access articles can be viewed online without a subscription.
www.plantcell.org/cgi/doi/10.1105/tpc.111.087874

analysis of a *WOX5* promoter-driven green fluorescent protein (GFP) reporter (*WOX5*$_{pro}$:*ERGFP*) and quantitative RT-PCR (qRT-PCR) analyses demonstrated that auxin negatively regulates *WOX5* expression in the distal root tip (Ding and Friml, 2010). Consistently, according to a *DR5*$_{pro}$:*GUS* reporter, auxin levels and distribution are not disturbed in *wox5* root tips (Sarkar et al., 2007), and ectopic *WOX5*$_{pro}$:*ERGFP* activity is observed in lines with reduced activity of ARF10 and ARF16 transcription factors, which mediate auxin signaling (Ding and Friml, 2010).

In the shoot apical meristem, *WUSCHEL* (*WUS*), the founding member of the *WOX* gene family, fulfills similar roles to *WOX5* in the RAM (Schoof et al., 2000). Expressed in the organizing center, *WUS* is essential for maintaining the meristematic state of distal stem cells, although analyses of *DR5*-driven reporters do not reveal an auxin maximum in the *WUS* expression domain (Smith et al., 2006). However, for somatic embryogenesis and de novo shoot induction, *WUS* expression is essential, and its induction depends strongly on the level of auxin (Gordon et al., 2007; Su et al., 2009). Furthermore, the specification of lateral organs, and the activity of the shoot apical meristem itself, are controlled by auxin and its regulated transport (Bayer et al., 2009; Prusinkiewicz et al., 2009). Thus, auxin plays an essential role in the activation and maintenance of stem cell niches in apical meristems upstream of *WOX* gene family members.

Recently, an essential role for the WOX4 transcription factor in promoting cambium activity was identified (Ji et al., 2010; Hirakawa et al., 2010). As for the function of *WUS* and *WOX5* in apical meristems, *WOX4* is crucial for the proliferating activity of the cambium. This observation revealed surprising parallels in the level of transcriptional regulators in the apical and lateral meristems despite major anatomical differences (Hirakawa et al., 2010). A functional *WOX4* gene is required for PHLOEM INTERCALATED WITH XYLEM (PXY) (also known as PUTATIVE TDIF RECEPTOR), a leucine-rich repeat receptor-like kinase, to function as a promoter of cambium proliferation. *PXY*, similar to *WOX4*, is expressed in the cambium (Fisher and Turner, 2007; Etchells and Turner, 2010; Hirakawa et al., 2010) and is bound and activated by CLE41/44, a member of the CLV3/ESR-related (CLE) peptide family (Ito et al., 2006; Hirakawa et al., 2008; Etchells and Turner, 2010). The current view is that the ligand is produced in the phloem ensuring communication between these (pro)cambium-derived cells and the cambium itself to balance tissue production and to orientate cell divisions (Hirakawa et al., 2008; Etchells and Turner, 2010).

In spite of extensive research on the auxin-cambium relationship, and in contrast with our knowledge about the effect of auxin on apical meristems, the molecular basis of the translation of basipetal auxin transport into the establishment and promotion of cambium activity is unknown. In this study, we dissect the interaction of *WOX4* with the auxin-dependent induction of cambium activity. Taking advantage of the inducibility of cambium activity in the *Arabidopsis thaliana* inflorescence shoot by local 1-*N*-naphthylphthalamic acid (NPA) treatments, we show that auxin-dependent stimulation of cambium activity depends on *WOX4* and its upstream regulator *PXY*, placing both factors genetically downstream of auxin signaling. Thereby, we reveal two essential factors involved in the translation of basipetal auxin transport into cambium activity by mediating auxin sensitivity to cambium cells and uncover parallels, but also differences, in how auxin regulates apical and lateral meristems.

RESULTS

Sites of Enhanced Auxin Signaling and *WOX4* Activity Are Distinct

To dissect the spatial and temporal relationship between high levels of auxin signaling and *WOX4* activity in cambium regulation, we introduced a *WOX4* reporter construct (*WOX4*$_{pro}$:*YFP* [for yellow fluorescent protein]) into a line carrying the *DR5rev*$_{pro}$:*GFP* reporter, which visualizes auxin signaling (Benková et al., 2003). The *WOX4*$_{pro}$:*YFP* reporter recapitulated the pattern of *WOX4* activity in the cambium of the hypocotyl and veins of cotyledons reported earlier (Figures 1A and 1B) (Hirakawa et al., 2010). Furthermore, a construct expressing *WOX4* under the control of the same promoter fragment (*WOX4*$_{pro}$:*WOX4*) was able to complement the defects caused by *WOX4*-deficiency (see below), suggesting that reporter activity reflects the activity of the endogenous *WOX4* promoter.

Initially, the activities of the *WOX4*$_{pro}$:*YFP* and *DR5rev*$_{pro}$:*GFP* reporters were analyzed at two different positions along the inflorescence stem. Ten millimeters above the uppermost rosette leaf, cambium identity is restricted to vascular bundles; thus, stem anatomy displays a primary pattern (Figures 1C, 1E, to 1G; see Supplemental Figure 1A online) (Sehr et al., 2010). At this position, *WOX4*$_{pro}$:*YFP* activity was detected in vascular bundles in cells that were identified as cambium cells based on their organization in typical radial cell files (Figures 1E to 1G; see Supplemental Figure 2A online). In comparison, *DR5rev*$_{pro}$:*GFP* activity was observed distally to sites with enhanced *WOX4*$_{pro}$:*YFP* activity toward the phloem and in the phloem itself (Figures 1E to 1G; see Supplemental Figure 2A online). In addition to primary bundles, *DR5rev*$_{pro}$:*GFP* activity was detected in single cortex cells in interfascicular regions (Figures 1F and 1G; see Supplemental Figure 2A online, green arrows). At the position of the uppermost rosette leaf, which for simplicity is denoted as stem base throughout the text (see Supplemental Figure 1A online), a continuous domain of cambium activity is present and stem anatomy has transformed into a secondary pattern (Figures 1D and 1H to 1J; see Supplemental Figure 2B online) (Sehr et al., 2010). Here, the activity of both reporters was observed in two distinct and continuous domains extending from vascular bundles into interfascicular regions (Figures 1I and 1J; see Supplemental Figure 2B online). An overlap of both activities was observed in individual cells at the border between both activity domains (Figures 1I and 1J; see Supplemental Figure 2B online, white arrows). Based on these observations, and the finding that the auxin-responsive *AtGH3.3*$_{pro}$:*GUS* reporter (Hagen et al., 1991; Mallory et al., 2005; Goda et al., 2008; Teichmann et al., 2008) is also active in phloem-related tissues in stems (see Supplemental Figures 3A and 3B online), we conclude that domains with elevated *WOX4* promoter activity and with elevated auxin signaling are mostly distinct in the context of the established cambium-specific stem cell niche in *Arabidopsis* stems.

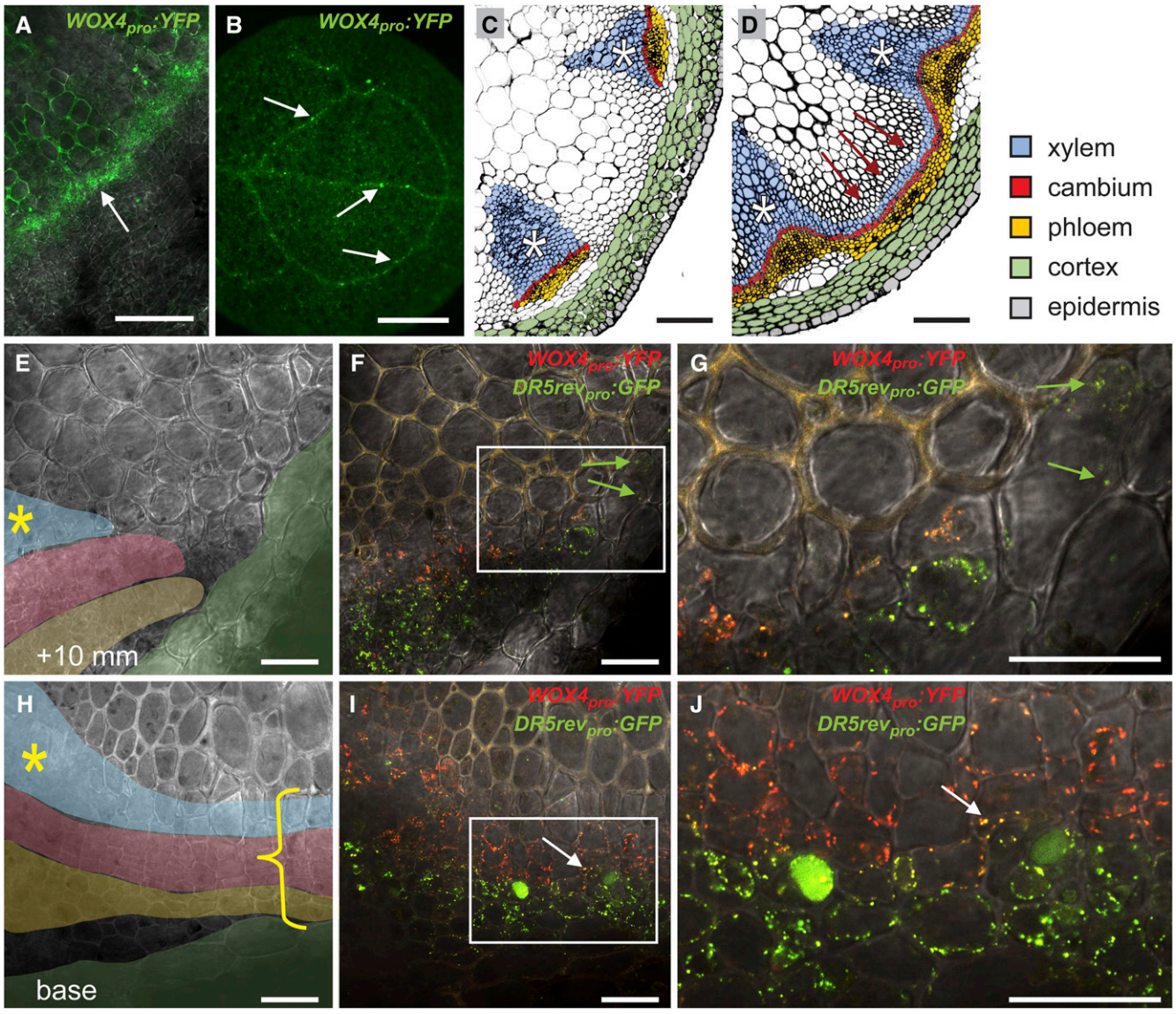

Figure 1. Comparison of *WOX4*$_{pro}$:*YFP* and *DR5rev*$_{pro}$:*GFP* Activities in the *Arabidopsis* Inflorescence Stem.

(A) and **(B)** *WOX4*$_{pro}$:*YFP* activity (arrows) in the hypocotyl of 30-cm-tall plants **(A)** and in cotyledons of 21-d-old seedlings **(B)**.
(C) and **(D)** Schematic representations of tissue patterns in primary (**[C]**; before onset of secondary growth) and secondary (**[D]**; after onset of secondary growth) stems. The IC is indicated by arrows.
(E) to **(J)** Analysis of reporter gene activity 10 mm above the uppermost rosette leaf (**[E]** to **[G]**) and at the stem base (**[H]** to **[J]**) of 30-cm-tall plants. Tissues are marked in **(E)** and **(H)** according to the color coding used in **(C)** and **(D)**. **(F)**, **(G)**, **(I)**, and **(J)** show overlays of the YFP- and GFP-specific channels with the respective bright-field image. Details shown in **(G)** and **(J)** are marked in **(F)** and **(I)**, respectively. The yellow bracket in **(H)** indicates the extension of the IC-derived tissue. *WOX4*$_{pro}$:*YFP* signal in red, *DR5rev*$_{pro}$:*GFP* signal in green (green arrows), and overlapping signal in yellow (white arrows).
Bars = 50 μm in **(A)**, 500 μm in **(B)**, 100 μm in **(C)** and **(D)**, and 25 μm **(E)** to **(J)**. The position of primary vascular bundles is indicated by asterisks. Note that autofluorescence of secondary cell walls generates background signals (cf. Supplemental Figure 3 online). The combination of the YFP- and GFP-specific channels shown in **(G)** and **(J)** is also depicted in magenta and green, respectively, in Supplemental Figure 2 online.

To characterize the early stages of cambium initiation, we concentrated on the formation of the interfascicular cambium (IC) and dissected the spatio-temporal relationship of both markers during this process. For this, we analyzed stems 5 mm above the stem base where the IC is initiated when shoots grow from 5 to 30 cm tall (Sehr et al., 2010). In 5-cm-tall stems, cambial activity was, together with *DR5rev*$_{pro}$:*GFP* and *WOX4*$_{pro}$:*YFP* activities, restricted to primary bundles (Figures 2A to 2C; see Supplemental Figure 4A online) (Sehr et al., 2010). Representing an intermediate stage, both reporter activities extended further into the interfascicular region of 15-cm-tall plants, reflecting IC initiation (Figures 2D to 2F; see Supplemental Figure 4B online).

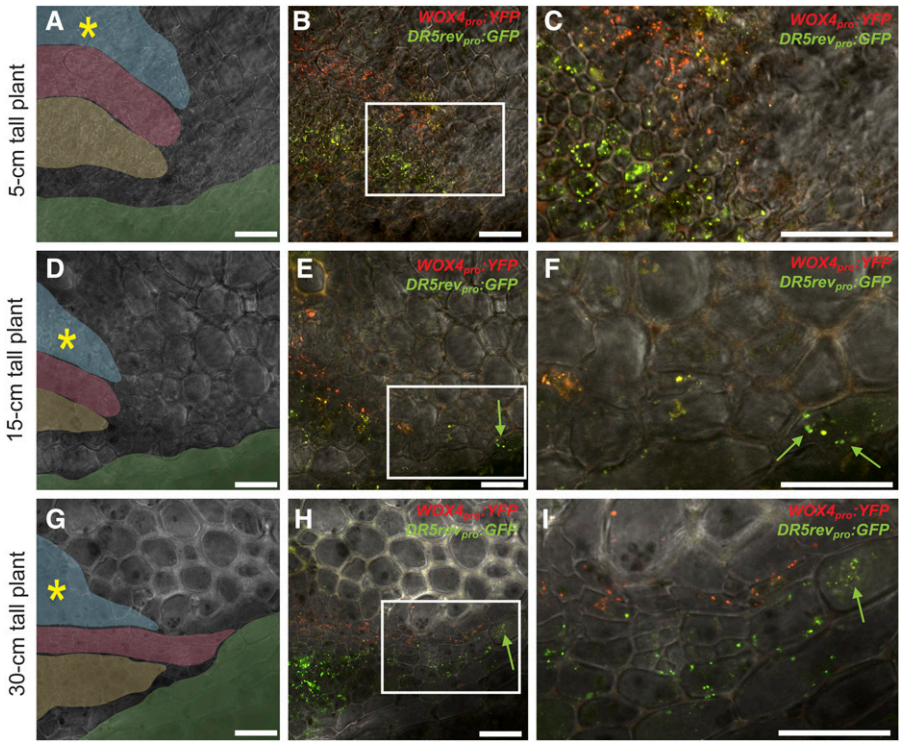

Figure 2. Analysis of *WOX4*$_{pro}$:*YFP* and *DR5rev*$_{pro}$:*GFP* Activities 5 mm above the Uppermost Rosette Leaf at Different Growth Stages.

(A) to **(C)** A 5-cm-tall plant.
(D) to **(F)** A 15-cm-tall plant.
(G) to **(I)** A 30-cm-tall plant.
(G), **(F)**, and **(I)** show details marked in **(B)**, **(H)**, and **(E)**, respectively. In the gray-channel images in **(A)**, **(D)**, and **(G)**, tissues are marked according to the color coding used in Figures 1C and 1D. *WOX4*$_{pro}$:*YFP* signal in red and *DR5rev*$_{pro}$:*GFP* signal in green (green arrows). Bars = 25 μm. The combination of the YFP- and GFP-specific channels shown in **(C)**, **(F)**, and **(I)** is also depicted in magenta and green, respectively, in Supplemental Figure 4 online.

In comparison to *DR5rev*$_{pro}$:*GFP* activity, *WOX4*$_{pro}$:*YFP* activity was detected closer to the bundle proximal to cells with high *DR5rev*$_{pro}$:*GFP* activity (Figures 2E and 2F; see Supplemental Figure 4B online). Importantly, in areas in which cell divisions are induced in this stage, *DR5rev*$_{pro}$:*GFP* but not *WOX4*$_{pro}$:*YFP* activity was found (Figure 2F; see Supplemental Figure 4B online, green arrows). In 30-cm-tall stems, *DR5rev*$_{pro}$:*GFP* and *WOX4*$_{pro}$:*YFP* activities were more prominent in interfascicular regions, again in mostly nonoverlapping domains (Figures 2G to 2I; see Supplemental Figure 4C online), resembling the situation at the position at the stem base (Figure 1I). These data show that the induction of *DR5rev*$_{pro}$:*GFP* activity represents a localized and early marker of IC activity preceding *WOX4*$_{pro}$:*YFP* activity during IC initiation.

WOX4 Is Essential for Cambium Activity in the Inflorescence Stem

WOX4 is an essential cambium regulator and a candidate for being the functional representative of the *WOX* gene family in the cambium-specific stem cell niche (Mayer et al., 1998; Sarkar et al., 2007; Hirakawa et al., 2010). To decipher the role of *WOX4* in cambium regulation in the inflorescence stem, we studied the *wox4-1* mutant, which is considered to carry a *WOX4* null allele (Hirakawa et al., 2010). We determined the activity of the fascicular cambium (FC) and of the IC by measuring the lateral extension of the cambium-derived tissue at the stem base and observed strongly reduced fascicular and IC activity in *wox4-1* (Figures 3A, 3B, and 3D). The expression of the *WOX4* open reading frame under the control of the *WOX4* promoter (*WOX4*$_{pro}$:*WOX4*) restored cambium activity, confirming that the promoter fragment used for our reporter constructs mediates gene activity resembling the activity of endogenous *WOX4* (Figures 3C and 3D). These findings show that, in addition to regulating cambium activity in the hypocotyl (Hirakawa et al., 2010), *WOX4* acts as a cambium regulator in the stem, supporting a general role for *WOX4* as an important cambium regulator throughout the plant body.

As with the hypocotyl (Hirakawa et al., 2010), our histological analyses indicated that cambium activity is not completely abolished in *wox4-1* stems, especially in the FC (Figure 3D). Consistent with a residual cambium activity in *wox4-1*, single cells predominantly in the FC accumulated histone *H4* mRNA, a marker for dividing cells (Barkoulas et al., 2008), demonstrating that they were actively dividing (Figure 3F). The domain of dividing cells overlapped with the domain of *WOX4* mRNA

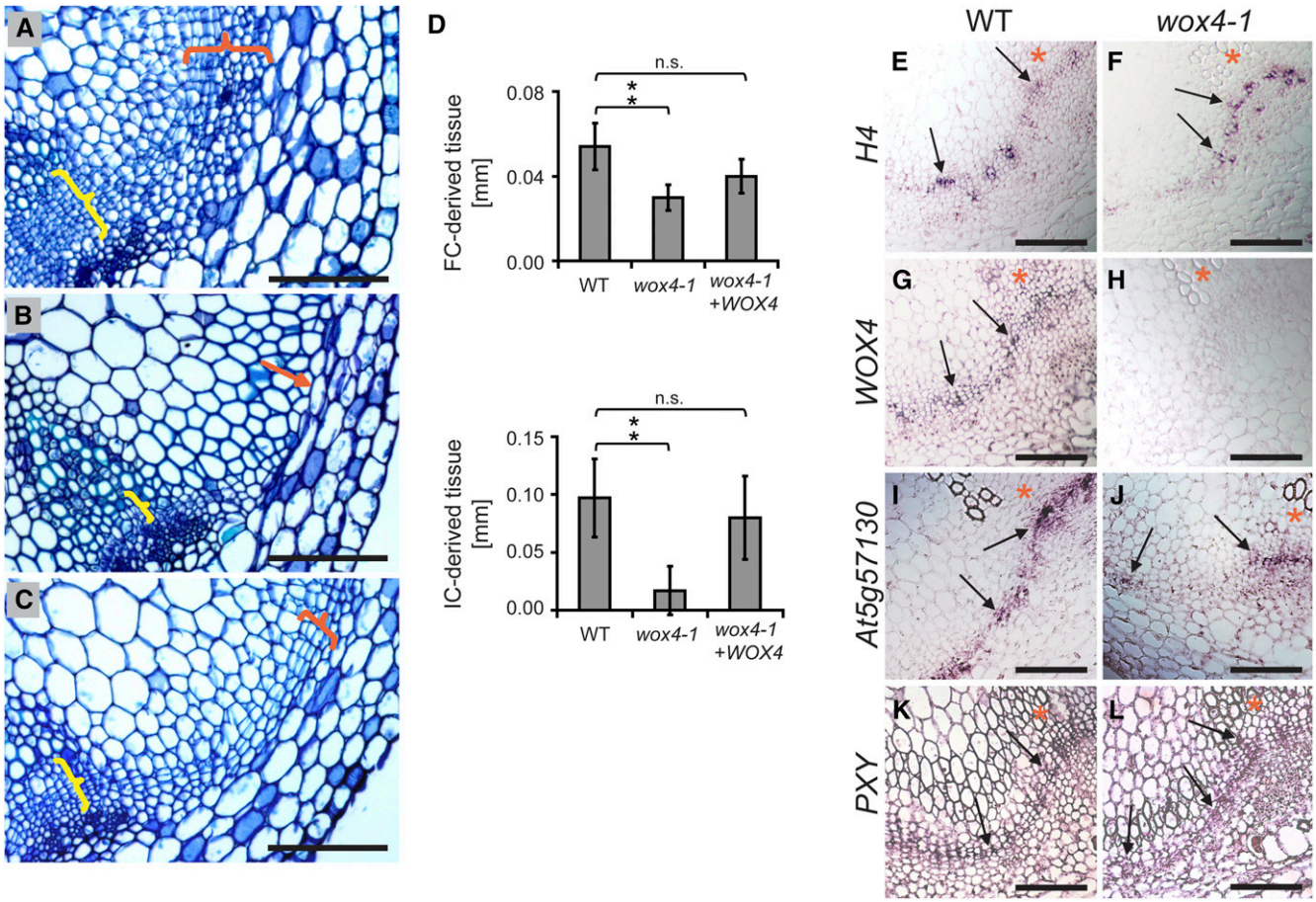

Figure 3. *WOX4* Is an Essential Factor for Cambium Activity in the Inflorescence Stem.

(A) to **(C)** Histological analysis of wild-type **(A)**, *wox4-1* **(B)**, and $WOX4_{pro}$:*WOX4*/*wox4-1* plants **(C)** at the stem base. Brackets indicate the lateral extensions of the IC-derived (red) or the FC-derived (yellow) tissue. The red arrow in **(B)** indicates the expected position of the IC.

(D) Quantitative analysis of cambium activity in wild-type, *wox4-1*, and $WOX4_{pro}$:*WOX4*/*wox4-1* plants. The extensions of the FC- and the IC-derived tissue were measured. Significance levels are calculated for the differences between the wild type and *wox4-1* and between the wild type and $WOX4_{pro}$:*WOX4*/*wox4-1* plants. n.s., not significant; double asterisks indicate significance levels of $P < 0.01$.

(E) to **(L)** Results of RNA in situ hybridization experiments using histone *H4* (**[E]** and **[F]**), *WOX4* (**[G]** and **[H]**), *At5g57130* (**[I]** and **[J]**), and *PXY* (**[K]** and **[L]**) specific antisense probes in the wild type (WT) (**[E]**, **[G]**, **[I]**, and **[K]**) and *wox4-1* (**[F]**, **[H]**, **[J]**, and **[L]**). Experiments were performed in 5-cm (*H4* and *WOX4* probes) and 15-cm (*At5g57130* and *PXY* probes) tall plants. Arrows indicate sites of mRNA accumulation, and asterisks label the position of primary vascular bundles. Bars = 100 μm.

accumulation (Figure 3G), suggesting that *WOX4* fulfills a cell-autonomous role in facilitating meristematic activity. Based on these results, we concluded that the establishment of cambium identity is not affected in *wox4-1* but that cambium activity is reduced.

To support this conclusion, we performed transcriptional profiling comparing *wox4-1* and wild-type stems. First, we compared stem fragments from 1.5 cm above the base (see Supplemental Figure 1B online), where hardly any anatomical differences between the wild type and *wox4-1* are observed, and detected just 29 genes with reduced transcript accumulation in *wox4-1* mutants (see Supplemental Data Set 1A online). The comparison of this group of genes with the group of 117 genes induced in cambium initiating cells (Agusti et al., 2011) revealed only one gene (*At2g28790*) present in both data sets (see Supplemental Data Set 1A online), supporting the idea that cambium identity is not impaired in *wox4-1* mutants. Next, we compared stem fragments from the stem base (see Supplemental Figure 1B online), in which the IC is initiated and a considerable amount of secondary vascular tissue is formed in wild-type but not in *wox4-1* plants. This comparison revealed 266 genes with reduced activity in *wox4-1* stems (see Supplemental Data Set 1B online) from which only five genes (1.9%) were classified as being cambium related (Agusti et al., 2011) (see Supplemental Data Set 1B online). By contrast, 45 genes (17%) were classified as being putatively cell cycle regulated or associated (Menges et al., 2003), and 72 genes (27%) were described as being preferentially expressed in the xylem (Zhao et al., 2005) (see

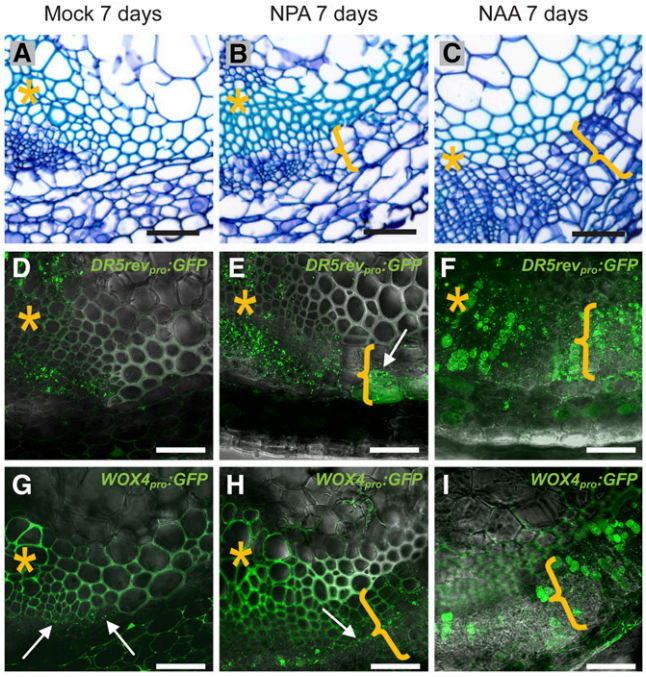

Figure 4. Comparison of the Effects of NPA and NAA Applied Locally to a Narrow Region of the Bottommost Elongated Internode of Wild-Type Plants.

(A) to **(C)** Toluidine-stained sections collected from the site of treatment showing the induction of periclinal cell divisions in interfascicular regions by NPA **(B)** and NAA **(C)** treatments.
(D) to **(F)** Activity of the *DR5rev$_{pro}$:GFP* reporter at the site of treatment.
(G) to **(I)** *WOX4$_{pro}$:GFP* reporter activity at the treatment site. The position of primary vascular bundles is indicated by asterisks. Arrows indicate sites of reporter gene activity. Extensions of the newly produced tissue are indicated by brackets. Bars = 50 μm.

Supplemental Data Set 1B online). The presence of the cambium-specific stem cell niche in *WOX4*-deficient plants was further confirmed by RNA in situ hybridization-based detection of the cambium-specific mRNAs encoded by *At5g57130* (Agusti et al., 2011) and *PXY* in the fascicular and interfascicular region of *wox4-1* plants (Figures 3I to 3L, sense control; see Supplemental Figure 5A online). Consistently, a *PXY$_{pro}$:GUS* reporter (Fisher and Turner, 2007) showed similar levels of activity in *wox4-1* mutant stems as in stems from wild-type plants (see Supplemental Figure 4B online). Taken together, these observations indicate that *WOX4* primarily affects the process of secondary growth by promoting cambium activity but not by establishing cambium identity.

WOX4 Is Crucial for the Auxin Responsiveness of the Cambium

To correlate *WOX4* activity and auxin signaling, we took advantage of the dependence of IC initiation on basipetal auxin transport and induced the IC in the bottommost elongated internode by local treatments with the auxin transport inhibitor NPA (see Supplemental Figure 1A online). This effect is based on the accumulation of basipetally transported auxin above the treatment zone (Sundberg et al., 1994; Little et al., 2002). To show that the effect is due to auxin accumulation, we initially compared NPA-treated stems with stems treated with the synthetic auxin analog 1-naphthaleneacetic acid (NAA) and observed similar effects with respect to the induction of cell divisions (Figures 4B and 4C). However, NPA treatments resulted in a pattern of *DR5rev$_{pro}$:GFP* activity more similar to the pattern at the stem base of untreated plants (Figures 4E and 4F, compare with Figure 1I), thus recapitulating the events observed during secondary growth initiation under natural conditions. This conclusion was also supported by a genome-wide transcriptional

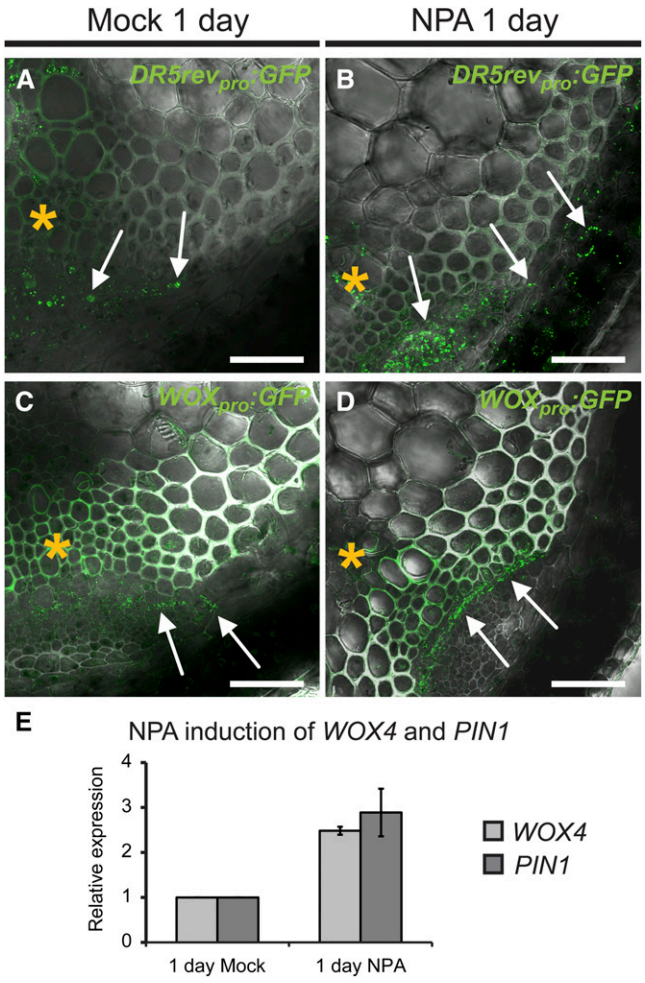

Figure 5. Short-Term Effect of Local NPA Treatments on *DR5rev$_{pro}$:GFP* and *WOX4$_{pro}$:GFP* Activities.

(A) and **(B)** *DR5rev$_{pro}$:GFP* activity in mock- **(A)** and NPA-treated **(B)** samples 1 d after treatment.
(C) and **(D)** *WOX4$_{pro}$:GFP* activity in mock- **(C)** and NPA-treated **(D)** samples. The position of primary vascular bundles is indicated by asterisks. Arrows indicate sites of reporter gene activity. Bars = 50 μm.
(E) qRT-PCR demonstrating that *WOX4* mRNA abundance is enhanced in stems after 1 d of NPA treatment, similar to *PIN1*. Two biological replicates with three technical replicates each were included.

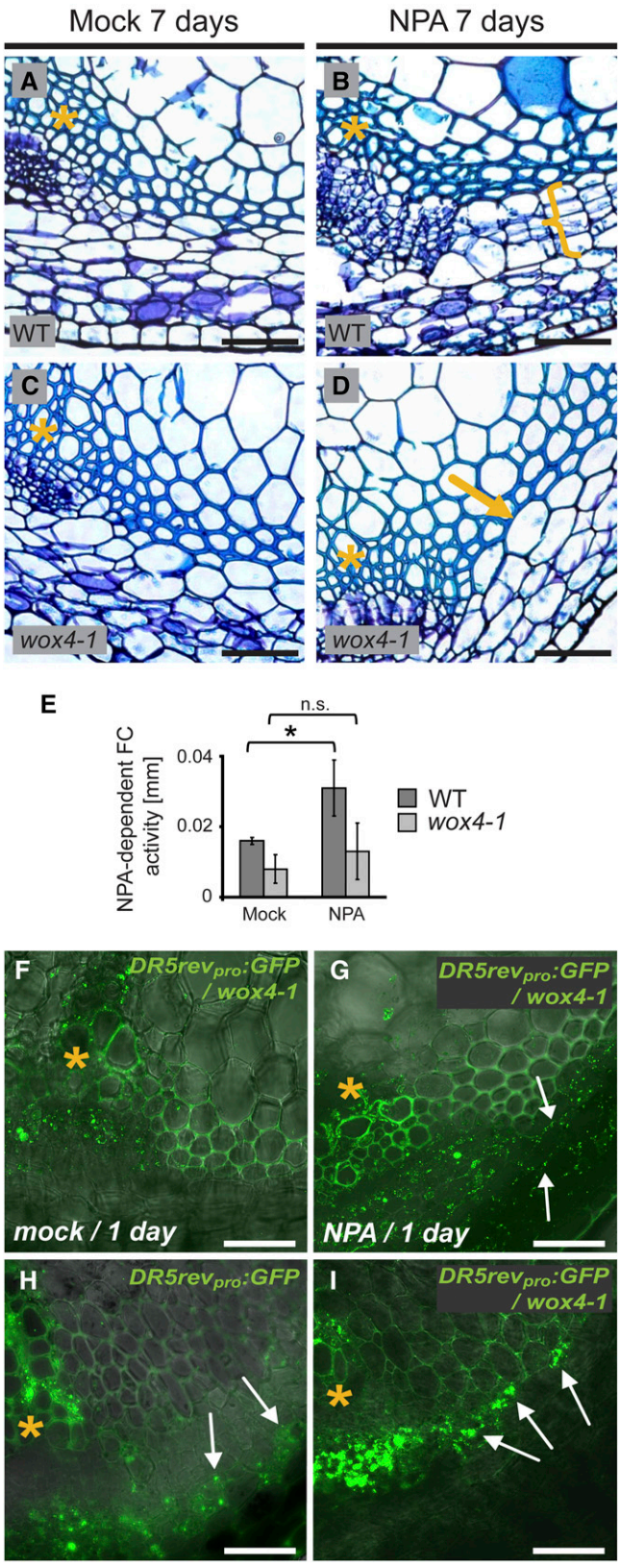

Figure 6. *WOX4* Is Essential for Auxin-Dependent Cambium Stimulation.

profiling comparing NPA-treated with mock-treated fragments, which led to the identification of 678 genes as being upregulated in response to NPA treatment (see Supplemental Data Set 2A online). When compared with the group of 117 genes induced during cambium-initiation identified previously (Agusti et al., 2011), we found that 24 (20.5%) of those are also NPA inducible, including the (pro)cambium markers *ATHB8*, *MOL1*, *RUL1*, and *PXY* (Agusti et al., 2011) (see Supplemental Data Set 2B online). Note that *WOX4* is not present on the ATH1 array used for these experiments. Given that only a 3.5% overlap was predicted based on a random selection of genes, these findings support the idea that localized auxin accumulation is important for IC initiation and that local NPA application allows us to mimic the natural initiation of cambium activity in *Arabidopsis* inflorescence stems.

To test the extent to which *WOX4* transcription itself is auxin dependent and reveal the dynamics of NPA-dependent change of *WOX4* activity on a cellular level, we treated stems of a *WOX4*$_{pro}$:*GFP* line with NPA, as described above. These treatments resulted in the induction of a GFP signal in a narrow domain in interfascicular regions (Figure 4H) resembling the pattern observed at the base of untreated stems (Figure 1I). The positive influence of auxin on *WOX4* activity in the stem was confirmed by qRT-PCR (Figure 8E; see Supplemental Figure 6A online) and by the inducibility of *WOX4*$_{pro}$:*GFP* activity by NAA treatments (Figure 4I). However, as for *DR5rev*$_{pro}$:*GFP*, the pattern of *WOX4*$_{pro}$:*GFP* activity was less defined in NAA-treated stems compared with NPA-treated stems (Figures 4H and 4I). NPA treatment of *WOX4*$_{pro}$:*GUS* and *DR5*$_{pro}$:*GUS* (Ulmasov et al., 1997) reporter lines locally induced reporter gene activities (see Supplemental Figures 6B to 6G online), demonstrating that, macroscopically, *WOX4* promoter activity correlates with enhanced auxin signaling.

To see what effect shorter periods of NPA treatment have on *DR5rev*$_{pro}$:*GFP* and *WOX4* activity, we analyzed plants 1 d after NPA application. At this point, no initiation of cell divisions was observed in interfascicular regions, but an increase of *DR5rev*$_{pro}$:*GFP* activity was detected in single cells in the area of future IC formation (Figures 5A and 5B). *WOX4*$_{pro}$:*GFP* activity was still restricted to vascular bundles; however, with enhanced activity compared with mock-treated samples (Figures 5C and 5D). Consistently, when tested by qRT-PCR, *WOX4* activity was

(A) to **(D)** In contrast with wild-type plants (**[A]** and **[B]**, bracket), *wox4-1* mutants (**[C]** and **[D]**) treated with NPA do not show enhanced FC activity **(D)** and no interfascicular cell divisions are induced (arrow in **[D]**).
(E) Quantification of the lateral extension of the FC-derived tissues did not reveal an effect of NPA treatment on FC activity in *wox4-1*. The asterisk indicates a significance level of $P < 0.05$. n.s., not significant; WT, wild type.
(F) and **(G)** In contrast with mock-treated stems **(F)**, *DR5rev*$_{pro}$:*GFP*/*wox4-1* stems treated for 1 d with NPA **(G)** display *DR5rev*$_{pro}$:*GFP* activity in cortex cells similarly to lines with a functional *WOX4* (arrows in **[G]**; see Figure 5B for comparison).
(H) and **(I)** Similarly to plants with a functional *WOX4* gene (arrows in **[H]**), *DR5rev*$_{pro}$:*GFP* activity is observed at the stem base in the interfascicular regions of *wox4-1* mutants (arrows in **[I]**). Asterisks mark the position of primary vascular bundles. Bars = 50 μm.

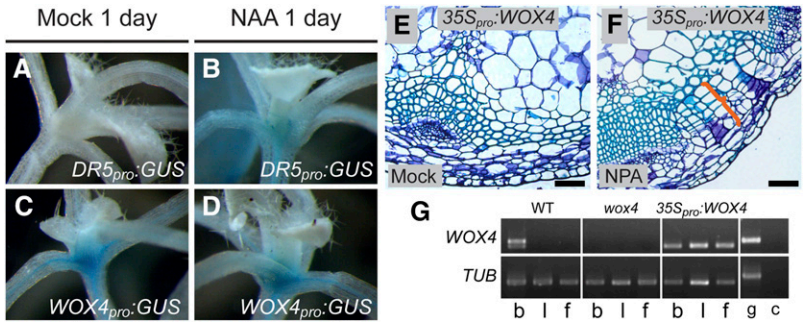

Figure 7. *WOX4* Promoter Activity and *WOX4*-Dependent Cambium Activation Depend on the Tissue Context.

(A) and **(B)** In comparison to mock treatment **(A)**, NAA treatment induces $DR5_{pro}$:*GUS* reporter gene activity **(B)** 1 d after treatment.
(C) and **(D)** No ectopic $WOX4_{pro}$:*GUS* reporter gene activity is observed upon NAA treatment.
(E) and **(F)** NPA treatment of $35S_{pro}$:*WOX4* stems **(F)** leads to wild-type-like IC initiation (cf. with Figures 4B and 6B). The IC-derived tissue is indicated by the bracket in **(F)**. Bars = 50 μm.
(G) RT-PCR comparing *WOX4* transcript abundance in the wild type (WT), *wox4-1*, and $35S_{pro}$:*WOX4*, at the stem base (b), in rosette leaves (l), and in flowers (f). Genomic DNA (g) and water (c) were used as control samples. Two technical replicates gave identical results.

enhanced in stems 1 d after treatment with NPA, similar to *PIN1* (Figure 5E), which is known to be auxin responsive (Goda et al., 2008). Collectively, these findings again support the idea that the induction of auxin signaling precedes the activation of *WOX4* activity in interfascicular regions and, furthermore, that *WOX4* activity within the FC is influenced by changes in auxin levels.

To test whether the temporal sequence of increased auxin signaling and *WOX4* activation during IC formation reflects a necessity of *WOX4* for auxin-dependent stimulation of cambium activity, we treated *wox4-1* plants with NPA. In contrast with the wild type, no cell divisions were induced in the interfascicular regions of *wox4-1* plants (Figures 6A to 6D) and the FC was not significantly activated (Figure 6E). This observation indicates that *WOX4* is essential for the positive effect of auxin on cambium activity and confirms a role for *WOX4* downstream of auxin in cambium regulation. If *WOX4* acts downstream of auxin signaling, the loss of *WOX4* function should not affect the activation of the *DR5* promoter by NPA treatments. To test this, we performed NPA treatments of $DR5rev_{pro}$:*GFP* plants harboring the *wox4-1* mutation. We observed the same effect as in plants with a functional *WOX4* gene after 1 d of treatment (Figures 6F and 6G, compare with Figure 5B). Also, at the base of $DR5rev_{pro}$:*GFP*/*wox4-1* stems, GFP-positive cells were observed in the interfascicular region (Figures 6H and 6I) even though IC initiation is severely affected. Collectively, these observations argue against a role for *WOX4* in promoting auxin accumulation.

Auxin-Dependent Cambium Stimulation Requires *PXY*

To see whether auxin is sufficient for inducing *WOX4* promoter activity in other parts of the plant, we treated seedlings of the $WOX4_{pro}$:*GUS* line with auxin. In contrast with the $DR5_{pro}$:*GUS* reporter (Figures 7A and 7B), we could not induce the $WOX4_{pro}$:*GUS* reporter ectopically by auxin treatment of seedlings (Figures 7C and 7D). Moreover, plants ectopically expressing *WOX4* resembled wild-type plants before and after NPA treatment with respect to stem tissue patterning and IC formation (Figures 7E to 7G). Therefore, we concluded that auxin-dependent cambium activation depends on the cellular context of the cambium-specific stem cell niche.

The leucine-rich repeat receptor-like kinase PXY has been reported to stimulate *WOX4* transcript accumulation (Hirakawa et al., 2010). *PXY* is expressed in cambium cells and is also essential for IC initiation at the base of the *Arabidopsis* stem (Agusti et al., 2011). To investigate whether *PXY*, in addition to *WOX4*, belongs to the repertoire of factors mediating auxin responsiveness to cambium cells, we treated *pxy-4* mutants (Fisher and Turner, 2007) with NPA as described above. Similar to *wox4-1*, no IC formation was observed in *pxy-4* (Figures 8A to 8D). Importantly, qRT-PCR did reveal an increase of *WOX4* transcript levels in the wild type and in two independent *pxy* mutants after 1 d of NPA treatment, indicating that the initial effect of auxin on *WOX4* activity is independent of *PXY*. By contrast, after 7 d of NPA treatment, *WOX4* mRNA levels were back to nontreated levels in *pxy* mutants, whereas there was a stable increase in the wild type (Figure 8E). Taken together, this suggests that the receptor-like kinase PXY is predominantly required for a stable auxin-dependent activation of *WOX4* activity and belongs to the repertoire of factors that translate auxin accumulation into the production of secondary vascular tissues.

DISCUSSION

Similar to apical plant meristems, the cambium in stems is under tight regulation of auxin signaling. In this study, we present data demonstrating a role for the *WUS* homolog *WOX4* as a key regulator of cambium activity in the main stem of *Arabidopsis* and reveal a requirement for *WOX4* and its upstream regulator *PXY* for the positive influence of auxin on cambium activity. This finding sheds light on the molecular pathway connecting auxin and cambium activity, a pathway for which, despite extensive investigation in the past (Snow, 1935; Sachs, 1981; Uggla et al., 1996; Schrader et al., 2003, 2004b), our current knowledge of the molecular events is scarce.

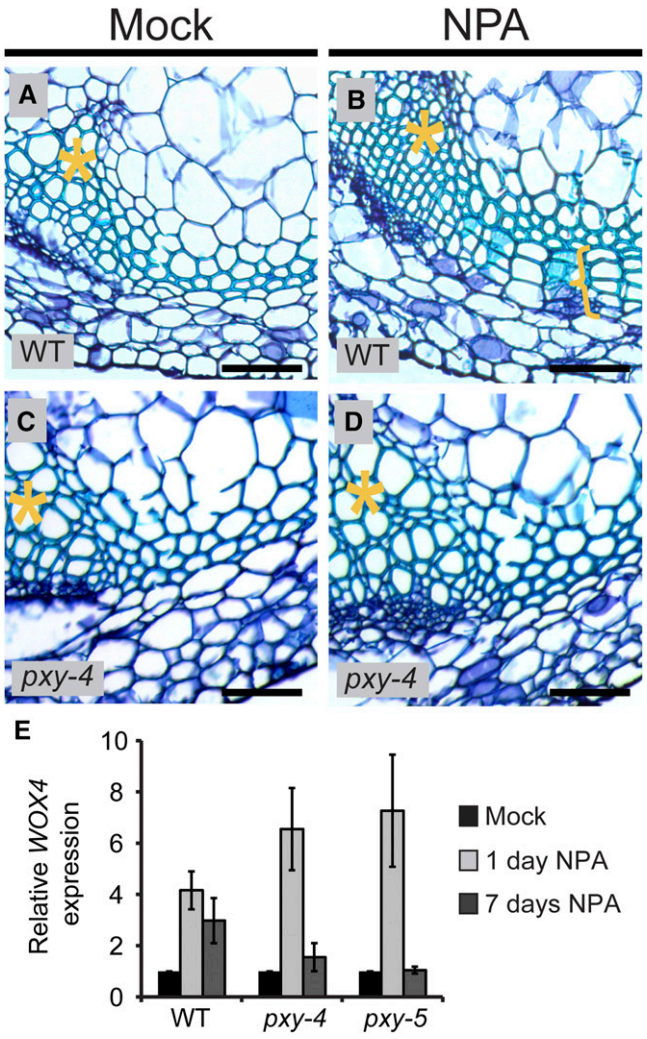

Figure 8. *PXY* Is Necessary for Auxin-Dependent Cambium Activation.

(A) to **(D)** In contrast with wild-type (WT) plants (**[A]** and **[B]**), *pxy-4* mutants (**[C]** and **[D]**) did not respond to NPA treatment by an increase of cambium activity.

(E) *WOX4* mRNA abundance was not elevated in *pxy* mutant backgrounds after 7 d of NPA treatment, although *WOX4* activation took place 1 d after treatment. Bars = 50 μm.

[See online article for color version of this figure.]

The *wox4-1* mutant showed severe defects in fascicular, as well as interfascicular, cambial growth in the main stem and did not establish a closed cambium cylinder. At first sight, this implies a role for *WOX4* in cambium initiation. However, there are several observations making it unlikely that *WOX4* functions as an initiator of cambium identity: (1) ectopic expression of *WOX4* does not lead to ectopic cambium formation (this study; Hirakawa et al., 2010); (2) cell divisions in the FC are not completely abolished in *wox4-1* mutants, suggesting that cambium identity can be established without *WOX4* function (this study; Hirakawa et al., 2010); (3) *WOX4* expression in the interfascicular regions is late in comparison to early markers visualizing the onset of IC identity; and (4) expression analyses of selected marker genes and genome-wide transcriptional profiling hardly identified any genes characteristically expressed in cells harboring cambium identity as being reduced in *wox4-1* (Fisher and Turner, 2007; Hirakawa et al., 2008; Agusti et al., 2011). Earlier studies have argued that IC formation depends on the activity of the FC (Little et al., 2002; Sehr et al., 2010). Therefore, we suggest, in agreement with recent studies (Hirakawa et al., 2010), that the failure in initiating the IC is a secondary effect of the reduced activity of the FC in *wox4* mutant backgrounds and that the primary role of *WOX4* is to promote cambium activity.

Strikingly, NPA-induced auxin accumulation in a *wox4-1* mutant background had no effect on cambium activity. This observation, in combination with the observation that NPA-induced auxin accumulation is not disturbed in *wox4-1* mutants, argues for a role for *WOX4* downstream of auxin signaling in cambium regulation. Therefore, the *wox4-1* mutant phenotype seems to specifically reflect the impact of auxin on the activity of an established cambium and, thus, separate genetically auxin-dependent stimulation of cambium activity from auxin-dependent formation of procambium strands (Scarpella et al., 2006; Wenzel et al., 2007). Whether auxin acts on the cambium solely by influencing the level of *WOX4* expression is questionable, as plants with enhanced *WOX4* activity ($35S_{pro}$:*WOX4*) neither show more cambium activity (Hirakawa et al., 2010) nor have a greater response to local NPA treatments. Taking this into consideration, we rather favor a model in which *WOX4* activity in cambium cells mediates auxin responsiveness to the stem cells present in the cambium.

Analogous to the *WUS* and *WOX5* expression in apical meristems, *WOX4* is expressed in a narrow domain within the cambial zone. Given that the cambium functions as a bifacial meristem and that a common one-cell-layer-wide source of secondary phloem and xylem tissues has been postulated (Larson, 1994), the detection of *WOX4* expression presumably visualizes the cambium proper. Within the cambial zone, the cambium itself is often difficult to identify by simple histological means (Larson, 1994); therefore, *WOX4* expression should serve as a robust and informative marker for cambium identity. Interestingly, according to the $WOX4_{pro}$:*YFP* marker, *WOX4* activity is usually not restricted to one cell layer within the cambial zone but is rather detected in one to three cells in the radial orientation (Figures 1J and 3G). As the number of $WOX4_{pro}$:*YFP*-positive cells varies between neighboring radial cell files (Figure 1J), this variation might reflect different time periods passed since new cells have been produced by *WOX4*-expressing cells and, thus, how far differentiation has proceeded in these cambium derivatives, which should lead to a gradual *WOX4* inactivation. The role of *WOX4* as a promoter of cambium activity is reminiscent of the function of *WOX5* in the RAM, which is likewise not important for specifying the quiescent center but rather for maintaining the stem cell characteristics of surrounding cells (Sarkar et al., 2007). Whether *WOX4*-expressing cells fulfill similar functions to the quiescent center in the root tip as a mitotically rather inactive population of cells stimulating the proliferation of adjacent stem cells, in this case maybe xylem and phloem mother cells, remains to be elucidated. For this, molecular markers with sufficient resolution to distinguish between different cell identities within

the cambial zone need to be established; likewise, cell division rates have to be determined at high spatial resolution. However, the more flexible anatomy within the cambial zone and the less restricted activity of the *WOX4*$_{pro}$:*YFP* reporter suggest that concepts described for root meristems cannot be copied one-to-one to the cambium.

In contrast with the current view of radial cambium patterning based on results obtained in trees, we found indications that maxima of auxin signaling do not overlap with *WOX4*-expressing cells and that they are found more in cells gaining or carrying phloem identity. Because *DR5* activity is a rather indirect way of visualizing auxin levels and is also influenced by other hormones (Nakamura et al., 2003), we confirmed our observations using the auxin-responsive *AtGH3.3*$_{pro}$:*GUS* reporter (Hagen et al., 1991). Although weak auxin signaling in *WOX4*-expressing cells might not be detectable by these markers, our data suggest that auxin accumulation has a rather indirect and non-cell-autonomous effect on *WOX4*-expressing cells.

The CLE41/44/PXY signaling module is a positive regulator of *WOX4* activity (Hirakawa et al., 2010) and, consistent with a role of the module also in the auxin-dependent cambium stimulation upstream of *WOX4*, NPA treatments of *pxy* mutants had no anatomical effect on cambium activity. The current picture is that the CLE41/44 peptide is produced in the phloem and then travels to the cambium, where it binds and activates the PXY receptor (Hirakawa et al., 2008, 2010; Etchells and Turner, 2010). According to the *DR5rev*$_{pro}$:*GFP* reporter, there is strong auxin signaling in the phloem; thus, it is tempting to speculate that the NPA-dependent induction of *WOX4* could be an indirect effect based on auxin accumulation in this tissue and the subsequent stimulation of CLE41/44 peptide production and/or traveling. However, the observation that initial *WOX4* activation is *PXY* independent and that enhanced *CLE41*, *CLE44*, or *CLE42* (a gene encoding a second putative PXY ligand) activity was not detected upon NPA treatment (see Supplemental Data Set 2A online) do not appear to support this possibility.

Taken together, by identifying a strong connection between *WOX4* and auxin signaling, we revealed a parallel between the regulation of the cambium and the regulation of apical meristems in which *WOX* gene function likewise depends on auxin signaling (Haecker et al., 2004; Su et al., 2009; Ding and Friml, 2010). Because plant meristem activity has to be coordinated with general plant growth and be adapted to changing environmental requirements, various inputs mediated by long- and short-range signaling have to be integrated on the level of the respective stem cells. Here, we show that *WOX4* is one essential factor that makes the cambium responsive to the long-distance regulation by auxin transported basipetally along the stem.

METHODS

Plant Material

All plant lines used in this study were *Arabidopsis thaliana* plants of the accession Columbia, except the *PXY*$_{pro}$:*GUS* reporter line, which has the Landsberg *erecta* background (Fisher and Turner, 2007). The *wox4-1* (GK_462GO1, N376572), *pxy-4* (SALK_009542, N800038), and *pxy-5* (SALK_002910, N502910) mutants, as well as the *DR5rev*$_{pro}$:*GFP* reporter line (N9361; Benková et al., 2003), were ordered from the Nottingham Arabidopsis Stock Centre (NASC). The *AtGH3.3*$_{pro}$:*GUS* reporter line was provided by Thomas J. Guilfoyle (University of Missouri, Columbia, MO).

Plant Growth and Histological Analyses

After 3 weeks of growth under short-day conditions (8 h light, 16 h dark), plants were transferred to long-day conditions (16 h light, 8 h dark) to induce flowering. Unless stated otherwise, analyses of the shoot base were performed in plants of 15 to 20 cm height that had a first internode of at least 3 cm in length (see Supplemental Figure 1A online). For histological analyses, stem segments of at least 1 cm in length were harvested and embedded in paraffin, sectioned, stained by toluidine blue (AppliChem), and analyzed as described previously (Sehr et al., 2010). Quantitative data were subjected to two-tailed independent Student's *t* tests using SPSS 18.0 software (http://www.spss.com). Significance levels of $P < 0.05$, $P < 0.01$, and $P < 0.001$ are indicated by single, double, and triple asterisks, respectively. Comparisons showing no significant difference are labeled accordingly. For the analysis of GFP reporter activity, rough hand sections were analyzed using an LSM 710 Zeiss spectral confocal microscope (Carl Zeiss), with an excitation at 488 nm and detection specifically at 499 to 512 nm (single marker lines). For analysis of the *DR5rev*$_{pro}$:*GFP WOX4*$_{pro}$:*YFP* double marker line, excitation at 488 nm and detection at 495 to 508 nm (GFP) and 524 to 543 nm (YFP), respectively, resulted in optimal resolution of the signals. Gray channel pictures were produced using the transmission photo multiplier detector (T-PMT) of the microscope. Wild-type autofluorescence images for GFP (detection at 499 to 512 nm) and YFP (detection at 524 to 543) are shown in Supplemental Figure 3 online.

NPA and NAA Treatment

Pure lanolin (Sigma-Aldrich) or lanolin containing 1% (w/w) NPA or 1% (w/w) NAA (both Duchefa Biochemie) was applied to the first internode of 15- to 20-cm-tall plants at a distance of at least 1.5 cm to the stem base, where, under natural conditions, no IC is formed (see Supplemental Figure 1A online) (Sehr et al., 2010). A ring of lanolin was placed around the stem, resulting in a treatment zone of 4 to 5 mm in its vertical dimension. After 1 or 7 d of incubation, stem segments were harvested and analyzed histologically as described above or used for RNA preparation. For testing the inducibility of *GUS* reporters by auxin, 10-d-old soil-grown seedlings were analyzed 24 h after spraying with 40 μM NAA (in 0.28% ethanol) or 0.28% ethanol, respectively. GUS reporter gene activity in seedlings was determined as described previously (Scarpella et al., 2006) without using acetone.

Transgenic Lines

The 3′ and 5′ promoter regions of *WOX4* were amplified from genomic DNA using the *WOX4for8*/*rev8* and *WOX4for2*/*rev2* primer pairs (see Supplemental Table 1 online). Both fragments were cloned into *pGreen0229* (Hellens et al., 2000) using *Kpn*I/*Bam*HI and *Bam*HI/*Sac*I restriction sites, respectively. The resulting plasmid (*pTOM49*) was used to produce the *WOX4*$_{pro}$:*YFP* (*pPS11*, using *ER-EYFP*), *WOX4*$_{pro}$:*GFP* (*pTOM53*, using *ER-mGFP5*), *WOX4*$_{pro}$:*GUS* (*pTOM51*), and *WOX4*$_{pro}$:*WOX4* (*pTOM54*) constructs by inserting fragments carrying the respective open reading frames. For generating the *35S*$_{pro}$:*WOX4* construct, the *WOX4* open reading frame was cloned into the *pGreen0229* vector containing the *35S* promoter. To avoid diffusion, all fluorescent proteins were targeted to the endoplasmatic reticulum (ER) by fusing them to the corresponding sequence motif (Haseloff et al., 1997). For establishing transgenic lines, constructs were transformed into wild-type plants, and several independent single-copy lines were identified by DNA gel blot

analyses. From those, lines with a strong and/or typical pattern of transgene activity were used for crossings and further analyses.

In Situ Hybridization

RNA in situ hybridizations, including H4 probe synthesis, were performed as described earlier (Greb et al., 2003; Sehr et al., 2010). For the *WOX4* probe, a fragment amplified from cDNA using the primers *WOX4for4*/*WOX4rev4* was cloned into the *pGEM-T* vector (Promega) and used as a template for transcription from the T7 or SP6 promoters. Similarly, the primers *At5g57130_for1*/*rev1* (Agusti et al., 2011) and *PXYfor7*/*rev7* (see Supplemental Table 1 online) were used for the construction of vectors carrying *At5g57130* or *PXY* fragments, respectively.

RNA Preparation and qRT-PCR

RNA was extracted from *Arabidopsis* by mixing frozen and ground plant material with 1 mL TRIZOL (Invitrogen). After centrifugation, 900 μL of the supernatant were transferred to a fresh tube, containing 200 μL of chloroform. Phases were separated by 15 min centrifugation at maximum speed in a benchtop centrifuge. Subsequently, the aqueous layer was added to 500 μL of isopropanol. RNA was precipitated at −20°C and, after centrifugation, the pellet was washed with 70% ethanol. RNA elution in RNase-free water was followed by treatment with RNase-free DNase and RNA-MiniElute column purification pursuant to the manufacturer's instructions (Qiagen). qRT-PCR was performed as described previously (Agusti et al., 2011). Normalization was done to *UBC28*, which showed stable expression throughout our microarray comparisons; for all qRT-PCRs, this led to the same results as the normalization to the alternative control *At3g12590* (Czechowski et al., 2005). Nonquantitative RT-PCR was performed in comparison to *TUBULIN*. All primers used for qRT-PCR are listed in Supplemental Table 1 online.

Transcriptional Profiling

For each condition, three biological replicates consisting of pools of 12 to 14 stem segments each were analyzed. Each stem segment had a length of 5 mm. For comparing *wox4-1* with the wild type, segments were collected from the stem base and from 1.5 cm above the base (see Supplemental Figure 1B online). For the analysis of the NPA effect, stems were treated as described above and harvested accordingly. Isolation of total RNA from stem segments was performed as described above. Before cDNA production, labeling, and hybridization by NASC's international Affymetrix service (ATH1 array; http://affymetrix.*Arabidopsis*.info), RNA quality was checked by gel electrophoresis and measurement of the $OD_{260:280}$ nm ratio. The robust multiarray method from the Bioconductor software package (Gentleman et al., 2004) was used for normalization and analysis of expression data. An adjusted P value of 0.05 and a $\log_2$ fold change of 0.5 were chosen as thresholds for selecting differentially expressed genes. A selection of four to six genes per comparison was chosen for microarray data validation by qRT-PCR, in all cases confirming the observed relative expression changes (see Supplemental Figure 7 online).

Accession Numbers

Microarray data produced in this study have been uploaded to the Gene Expression Omnibus (GEO) database (Barrett et al., 2009) and are accessible through GEO Series accession numbers GSE24763 (http://www.ncbi.nlm.nih.gov/geo/query/acc.cgi?acc=GSE24763) and GSE24781 (http://www.ncbi.nlm.nih.gov/geo/query/acc.cgi?acc=GSE24781). *WOX4*, *PXY*, *H4*, *GH3.3*, and *UBC28* correspond to the Arabidopsis Genome Initiative locus identifiers *At1g46480*, *At5g61480*, *At2g28740*, *At2g23170*, and *At1g64230*, respectively. *TUB* corresponds *to At5g62690* and *At5g62700*. Locus identifiers corresponding to genes found to be differentially expressed in microarray experiments are listed in Supplemental Data Sets 1 and 2 online.

Supplemental Data

The following materials are available in the online version of this article.

Supplemental Figure 1. Schematic Representation of the Regions along the Inflorescence Stem Analyzed in This Study.

Supplemental Figure 2. Two-Channel Overlays of the $WOX4_{pro}$:*YFP* and $DR5rev_{pro}$:*GFP* Images Shown in Figures 1G and 1J.

Supplemental Figure 3. $AtGH3.3_{pro}$:*GUS* Activity in Stems and Autofluorescence Detected in the GFP- and YFP-Specific Channels Used for Analysis of *DR5* and *WOX4* Promoter Activities.

Supplemental Figure 4. Two-Channel Overlays of the $WOX4_{pro}$:*YFP* and $DR5rev_{pro}$:*GFP* Images Shown in Figures 2C, 2F, and 2I.

Supplemental Figure 5. Sense Control for in Situ Hybridizations, and PXY_{pro}:*GUS* Expression in *wox4-1*.

Supplemental Figure 6. qRT-PCR Analysis of *WOX4* Transcript Accumulation in NAA-Treated Stems and $DR5_{pro}$:*GUS* and $WOX4_{pro}$:*GUS* Activity upon NPA Treatments.

Supplemental Figure 7. Microarray Data Validation by qRT-PCR.

Supplemental Table 1. Primers Used in This Study.

Supplemental Data Set 1. Genes Less Active in *wox4-1* in Comparison to the Wild Type.

Supplemental Data Set 2. Genes Induced by NPA Treatments.

ACKNOWLEDGMENTS

We thank Wolfgang Busch (Gregor Mendel Institute, Vienna, Austria) and Stephan Wenkel (University of Tübingen, Germany) and members of the Greb lab for helpful comments on the manuscript. The $DR5_{pro}$:*GUS* reporter line was provided by Christian Luschnig (University of Applied Life Sciences and Natural Resources, Vienna, Austria), the PXY_{pro}:*GUS* reporter line by Simon Turner (University of Manchester, UK), and the $AtGH3.3_{pro}$:*GUS* line by Thomas J. Guilfoyle (University of Missouri, Columbia, MO). This study was supported by grants of the Austrian Science Fund (FWF; P20728-B03 for S.S. and P21258-B03 for J.A. and M.S.).

AUTHOR CONTRIBUTIONS

S.S. and T.G. designed the research, and S.S., J.A., P.S., and M.S. performed the research. S.S., J.A., and T.G. analyzed the data, and S.S. and T.G. wrote the article.

Received June 2, 2011; revised August 4, 2011; accepted September 6, 2011; published September 16, 2011.

REFERENCES

Agusti, J., Lichtenberger, R., Schwarz, M., Nehlin, L., and Greb, T. (2011). Characterization of transcriptome remodeling during cambium formation identifies MOL1 and RUL1 as opposing regulators of secondary growth. PLoS Genet. **7:** e1001312.

Baba, K., Karlberg, A., Schmidt, J., Schrader, J., Hvidsten, T.R.,

Bako, L., and Bhalerao, R.P. (2011). Activity-dormancy transition in the cambial meristem involves stage-specific modulation of auxin response in hybrid aspen. Proc. Natl. Acad. Sci. USA **108:** 3418–3423.

Barkoulas, M., Hay, A., Kougioumoutzi, E., and Tsiantis, M. (2008). A developmental framework for dissected leaf formation in the Arabidopsis relative *Cardamine hirsuta*. Nat. Genet. **40:** 1136–1141.

Barrett, T., et al. (2009). NCBI GEO: Archive for high-throughput functional genomic data. Nucleic Acids Res. **37**(Database issue): D885–D890.

Bayer, E.M., Smith, R.S., Mandel, T., Nakayama, N., Sauer, M., Prusinkiewicz, P., and Kuhlemeier, C. (2009). Integration of transport-based models for phyllotaxis and midvein formation. Genes Dev. **23:** 373–384.

Benková, E., Michniewicz, M., Sauer, M., Teichmann, T., Seifertová, D., Jürgens, G., and Friml, J. (2003). Local, efflux-dependent auxin gradients as a common module for plant organ formation. Cell **115:** 591–602.

Björklund, S., Antti, H., Uddestrand, I., Moritz, T., and Sundberg, B. (2007). Cross-talk between gibberellin and auxin in development of Populus wood: Gibberellin stimulates polar auxin transport and has a common transcriptome with auxin. Plant J. **52:** 499–511.

Blilou, I., Xu, J., Wildwater, M., Willemsen, V., Paponov, I., Friml, J., Heidstra, R., Aida, M., Palme, K., and Scheres, B. (2005). The PIN auxin efflux facilitator network controls growth and patterning in Arabidopsis roots. Nature **433:** 39–44.

Czechowski, T., Stitt, M., Altmann, T., Udvardi, M.K., and Scheible, W.R. (2005). Genome-wide identification and testing of superior reference genes for transcript normalization in Arabidopsis. Plant Physiol. **139:** 5–17.

Ding, Z., and Friml, J. (2010). Auxin regulates distal stem cell differentiation in Arabidopsis roots. Proc. Natl. Acad. Sci. USA **107:** 12046–12051.

Elo, A., Immanen, J., Nieminen, K., and Helariutta, Y. (2009). Stem cell function during plant vascular development. Semin. Cell Dev. Biol. **20:** 1097–1106.

Etchells, J.P., and Turner, S.R. (2010). The PXY-CLE41 receptor ligand pair defines a multifunctional pathway that controls the rate and orientation of vascular cell division. Development **137:** 767–774.

Fisher, K., and Turner, S. (2007). PXY, a receptor-like kinase essential for maintaining polarity during plant vascular-tissue development. Curr. Biol. **17:** 1061–1066.

Friml, J., Benková, E., Blilou, I., Wisniewska, J., Hamann, T., Ljung, K., Woody, S., Sandberg, G., Scheres, B., Jürgens, G., and Palme, K. (2002). AtPIN4 mediates sink-driven auxin gradients and root patterning in Arabidopsis. Cell **108:** 661–673.

Gentleman, R.C., et al. (2004). Bioconductor: open software development for computational biology and bioinformatics. Genome Biol. **5:** R80.

Goda, H., et al. (2008). The AtGenExpress hormone and chemical treatment data set: Experimental design, data evaluation, model data analysis and data access. Plant J. **55:** 526–542.

Gordon, S.P., Heisler, M.G., Reddy, G.V., Ohno, C., Das, P., and Meyerowitz, E.M. (2007). Pattern formation during de novo assembly of the Arabidopsis shoot meristem. Development **134:** 3539–3548.

Greb, T., Clarenz, O., Schäfer, E., Müller, D., Herrero, R., Schmitz, G., and Theres, K. (2003). Molecular analysis of the LATERAL SUPPRESSOR gene in Arabidopsis reveals a conserved control mechanism for axillary meristem formation. Genes Dev. **17:** 1175–1187.

Haecker, A., Gross-Hardt, R., Geiges, B., Sarkar, A., Breuninger, H., Herrmann, M., and Laux, T. (2004). Expression dynamics of WOX genes mark cell fate decisions during early embryonic patterning in *Arabidopsis thaliana*. Development **131:** 657–668.

Hagen, G., Martin, G., Li, Y., and Guilfoyle, T.J. (1991). Auxin-induced expression of the soybean GH3 promoter in transgenic tobacco plants. Plant Mol. Biol. **17:** 567–579.

Haseloff, J., Siemering, K.R., Prasher, D.C., and Hodge, S. (1997). Removal of a cryptic intron and subcellular localization of green fluorescent protein are required to mark transgenic Arabidopsis plants brightly. Proc. Natl. Acad. Sci. USA **94:** 2122–2127.

Hellens, R.P., Edwards, E.A., Leyland, N.R., Bean, S., and Mullineaux, P.M. (2000). pGreen: A versatile and flexible binary Ti vector for Agrobacterium-mediated plant transformation. Plant Mol. Biol. **42:** 819–832.

Hirakawa, Y., Kondo, Y., and Fukuda, H. (2010). TDIF peptide signaling regulates vascular stem cell proliferation via the WOX4 homeobox gene in *Arabidopsis*. Plant Cell **22:** 2618–2629.

Hirakawa, Y., Shinohara, H., Kondo, Y., Inoue, A., Nakanomyo, I., Ogawa, M., Sawa, S., Ohashi-Ito, K., Matsubayashi, Y., and Fukuda, H. (2008). Non-cell-autonomous control of vascular stem cell fate by a CLE peptide/receptor system. Proc. Natl. Acad. Sci. USA **105:** 15208–15213.

Ito, Y., Nakanomyo, I., Motose, H., Iwamoto, K., Sawa, S., Dohmae, N., and Fukuda, H. (2006). Dodeca-CLE peptides as suppressors of plant stem cell differentiation. Science **313:** 842–845.

Ji, J., Strable, J., Shimizu, R., Koenig, D., Sinha, N., and Scanlon, M.J. (2010). WOX4 promotes procambial development. Plant Physiol. **152:** 1346–1356.

Ko, J.H., Han, K.H., Park, S., and Yang, J. (2004). Plant body weight-induced secondary growth in Arabidopsis and its transcription phenotype revealed by whole-transcriptome profiling. Plant Physiol. **135:** 1069–1083.

Larson, P.R. (1994). The Vascular Cambium: Development and Structure. (Berlin: Springer-Verlag).

Little, C.H.A., MacDonald, J.E., and Olsson, O. (2002). Involvement of indole-3-acetic acid in fascicular and interfascicular cambial growth and interfascicular extraxylary fiber differentiation in *Arabidopsis thaliana* inflorescence stems. Int. J. Plant Sci. **163:** 519–529.

Mallory, A.C., Bartel, D.P., and Bartel, B. (2005). MicroRNA-directed regulation of *Arabidopsis* AUXIN RESPONSE FACTOR17 is essential for proper development and modulates expression of early auxin response genes. Plant Cell **17:** 1360–1375.

Mayer, K.F., Schoof, H., Haecker, A., Lenhard, M., Jürgens, G., and Laux, T. (1998). Role of WUSCHEL in regulating stem cell fate in the Arabidopsis shoot meristem. Cell **95:** 805–815.

Menges, M., Hennig, L., Gruissem, W., and Murray, J.A. (2003). Genome-wide gene expression in an Arabidopsis cell suspension. Plant Mol. Biol. **53:** 423–442.

Nakamura, A., Higuchi, K., Goda, H., Fujiwara, M.T., Sawa, S., Koshiba, T., Shimada, Y., and Yoshida, S. (2003). Brassinolide induces IAA5, IAA19, and DR5, a synthetic auxin response element in Arabidopsis, implying a cross talk point of brassinosteroid and auxin signaling. Plant Physiol. **133:** 1843–1853.

Nilsson, J., Karlberg, A., Antti, H., Lopez-Vernaza, M., Mellerowicz, E., Perrot-Rechenmann, C., Sandberg, G., and Bhalerao, R.P. (2008). Dissecting the molecular basis of the regulation of wood formation by auxin in hybrid aspen. Plant Cell **20:** 843–855.

Petersson, S.V., Johansson, A.I., Kowalczyk, M., Makoveychuk, A., Wang, J.Y., Moritz, T., Grebe, M., Benfey, P.N., Sandberg, G., and Ljung, K. (2009). An auxin gradient and maximum in the *Arabidopsis* root apex shown by high-resolution cell-specific analysis of IAA distribution and synthesis. Plant Cell **21:** 1659–1668.

Prusinkiewicz, P., Crawford, S., Smith, R.S., Ljung, K., Bennett, T., Ongaro, V., and Leyser, O. (2009). Control of bud activation by an auxin transport switch. Proc. Natl. Acad. Sci. USA **106:** 17431–17436.

Sabatini, S., Beis, D., Wolkenfelt, H., Murfett, J., Guilfoyle, T.,

Malamy, J., Benfey, P., Leyser, O., Bechtold, N., Weisbeek, P., and Scheres, B. (1999). An auxin-dependent distal organizer of pattern and polarity in the Arabidopsis root. Cell **99:** 463–472.

Sachs, T. (1981). The control of the patterned differentiation of vascular tissues. Adv. Bot. Res. **9:** 151–162.

Sarkar, A.K., Luijten, M., Miyashima, S., Lenhard, M., Hashimoto, T., Nakajima, K., Scheres, B., Heidstra, R., and Laux, T. (2007). Conserved factors regulate signalling in *Arabidopsis thaliana* shoot and root stem cell organizers. Nature **446:** 811–814.

Scarpella, E., Marcos, D., Friml, J., and Berleth, T. (2006). Control of leaf vascular patterning by polar auxin transport. Genes Dev. **20:** 1015–1027.

Schoof, H., Lenhard, M., Haecker, A., Mayer, K.F., Jürgens, G., and Laux, T. (2000). The stem cell population of Arabidopsis shoot meristems in maintained by a regulatory loop between the CLAVATA and WUSCHEL genes. Cell **100:** 635–644.

Schrader, J., Baba, K., May, S.T., Palme, K., Bennett, M., Bhalerao, R.P., and Sandberg, G. (2003). Polar auxin transport in the wood-forming tissues of hybrid aspen is under simultaneous control of developmental and environmental signals. Proc. Natl. Acad. Sci. USA **100:** 10096–10101.

Schrader, J., Moyle, R., Bhalerao, R., Hertzberg, M., Lundeberg, J., Nilsson, P., and Bhalerao, R.P. (2004a). Cambial meristem dormancy in trees involves extensive remodelling of the transcriptome. Plant J. **40:** 173–187.

Schrader, J., Nilsson, J., Mellerowicz, E., Berglund, A., Nilsson, P., Hertzberg, M., and Sandberg, G. (2004b). A high-resolution transcript profile across the wood-forming meristem of poplar identifies potential regulators of cambial stem cell identity. Plant Cell **16:** 2278–2292.

Sehr, E.M., Agusti, J., Lehner, R., Farmer, E.E., Schwarz, M., and Greb, T. (2010). Analysis of secondary growth in the Arabidopsis shoot reveals a positive role of jasmonate signalling in cambium formation. Plant J. **63:** 811–822.

Smith, R.S., Guyomarc'h, S., Mandel, T., Reinhardt, D., Kuhlemeier, C., and Prusinkiewicz, P. (2006). A plausible model of phyllotaxis. Proc. Natl. Acad. Sci. USA **103:** 1301–1306.

Snow, R. (1935). Activation of cambial growth by pure hormones. New Phytol. **34:** 347–360.

Su, Y.H., Zhao, X.Y., Liu, Y.B., Zhang, C.L., O'Neill, S.D., and Zhang, X.S. (2009). Auxin-induced WUS expression is essential for embryonic stem cell renewal during somatic embryogenesis in Arabidopsis. Plant J. **59:** 448–460.

Sundberg, B., Tuominen, H., and Little, C. (1994). Effects of the indole-3-acetic acid (IAA) transport inhibitors N-1-naphthylphthalamic acid and morphactin on endogenous IAA dynamics in relation to compression wood formation in 1-year-old *Pinus sylvestris* (L.) shoots. Plant Physiol. **106:** 469–476.

Teichmann, T., Bolu-Arianto, W.H., Olbrich, A., Langenfeld-Heyser, R., Göbel, C., Grzeganek, P., Feussner, I., Hänsch, R., and Polle, A. (2008). GH3:GUS reflects cell-specific developmental patterns and stress-induced changes in wood anatomy in the poplar stem. Tree Physiol. **28:** 1305–1315.

Uggla, C., Mellerowicz, E.J., and Sundberg, B. (1998). Indole-3-acetic acid controls cambial growth in scots pine by positional signaling. Plant Physiol. **117:** 113–121.

Uggla, C., Moritz, T., Sandberg, G., and Sundberg, B. (1996). Auxin as a positional signal in pattern formation in plants. Proc. Natl. Acad. Sci. USA **93:** 9282–9286.

Ulmasov, T., Murfett, J., Hagen, G., and Guilfoyle, T.J. (1997). Aux/IAA proteins repress expression of reporter genes containing natural and highly active synthetic auxin response elements. Plant Cell **9:** 1963–1971.

Wenzel, C.L., Schuetz, M., Yu, Q., and Mattsson, J. (2007). Dynamics of MONOPTEROS and PIN-FORMED1 expression during leaf vein pattern formation in *Arabidopsis thaliana*. Plant J. **49:** 387–398.

Zhao, C., Craig, J.C., Petzold, H.E., Dickerman, A.W., and Beers, E.P. (2005). The xylem and phloem transcriptomes from secondary tissues of the Arabidopsis root-hypocotyl. Plant Physiol. **138:** 803–818.